Progress In Electromagnetics Research C, Vol. 25, 133–144, 2012

AN ULTRA-WIDEBAND BALANCED BANDPASS FILTER BASED ON DEFECTED GROUND STRUCTURES

B. Xia[1, 2, *], L.-S. Wu[2], and J. F. Mao[2]

[1]Zhenjiang Watercraft College PLA, Zhenjiang, Jiangsu 212003, China

[2]Key Lab of Ministry of Education for Research of Design and EMC of High Speed Electronic Systems, Shanghai Jiao Tong University, Shanghai 200240, China

Abstract—An ultra-wideband (UWB) balanced bandpass filter (BPF) is proposed and designed using defected ground structures (DGSs). A multimode resonator on top layer with a coplanar waveguide on bottom layer is used to design a UWB BPF. U-shaped and H-shaped DGSs loaded with capacitor are used to design to provide common mode rejection within a lower band, while a set of dumbbell-shaped DGSs are utilized to provide common mode rejection within an upper-band. The proposed UWB balanced BPF shows the performance of good common mode rejection in and out of the UWB passband.

1. INTRODUCTION

With the development of fully-integrated balanced transceiver, differential-mode operation exhibits much higher immunity to noise than single-ended signaling. Much effort has been made to develop various balanced filters to meet the requirement of common-mode suppression in modern high-speed communication systems.

In [1], a balanced bandpass filter (BPF) is implemented with balanced coupled-line structures. In [2], half- and quarter-wavelength stepped-impedance resonators (SIRs) are utilized to realize dual-band balanced BPF. Both the two balanced BPFs have narrow differential-mode passband and wide common-mode suppression band. The center loading technique is proposed to further improve the common-mode suppression characteristic for narrowband BPFs [3]. In [4], a

Received 25 August 2011, Accepted 8 November 2011, Scheduled 14 November 2011

* Corresponding author: Bin Xia (xiabinsjtu@163.com).

compact second-order differential bandpass filter is presented. The transformer structure is integrated using integrated passive device (IPD) technology on a glass substrate to achieve compact circuit area and system-in-package (SiP) applications. In [5], a very compact differential bandpass filter was designed with improved high-frequency rejection, suitable for SiP circuit integration.

Ultra-wideband (UWB) technique has drawn much attention for various applications [6–9]. A two-stage differential-mode BPF is designed using symmetrical bisections of branch-line topology [10]. A six-stage UWB differential-mode BPF is implemented [11], but with poor performance of in-band insertion loss. In [12], the equivalent $3\lambda/4$ short-ended stub is introduced into a wideband differential-mode BPF to achieve good frequency selectivity. In [10–12], however, the common-mode suppression in stopband is not good, and the out-of-band common-mode noise would still produce possible electromagnetic interference (EMI) problem for wireless application. In [13], an UWB differential filter is developed with good performance of differential-mode propagation and common-mode suppression, which is based on the structure of double-side parallel-strip line (DSPSL). However, in order to incorporate the DSPSL structure into widely used microstrip circuit, additional transitions are needed to accomplish their connection, which may take more area and introduce more losses.

In this article, a novel UWB balanced BPF is proposed with a pair of symmetrical UWB filtering units based on differential transmission lines. To improve its performance of common-mode suppression, dumbbell-, U- and H-shaped defected ground structures (DGSs) are introduced to reject the common-mode propagation from DC to 18 GHz. The good performance of our proposed UWB balanced BPF with DGSs has been demonstrated by the agreement obtained between the simulated and measured S-parameters.

2. ANALYSIS AND DESIGN

The top and bottom views of the proposed UWB balanced BPF are shown in Figs. 1(a) and (b), respectively. It is mainly composed of three parts. The first part is a pair of UWB filtering units designed for differential transmission lines. The second part is built up by two U-shaped DGSs and an H-shaped one loaded with a capacitor. These three etched structures provide the rejection of common-mode noise within the lower band of UWB. The third part consists of a set of dumbbell-shaped DGSs to suppress the common-mode noise in upper band of UWB. Odd mode impedance of differential line matching to $50\,\Omega$, and is computed by the methods about coupled microstrip

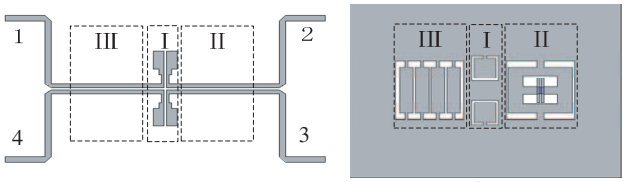

Figure 1. Configuration of the proposed UWB balanced BPF. (a) Its top view, and (b) bottom view.

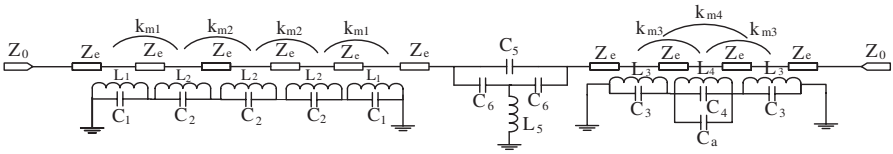

Figure 2. The common mode equivalent lumped model.

without considering DGS, that is because DGS has little influence on odd mode impedance in passband. Even mode impedance mismatch with 50 Ω, mismatching benefit to suppress common mode noise, the DGS of Sections 2 and 3 suppress mainly common mode noise. So, even mode impedance may not need to be considered.

2.1. Theoretical Model and Parameters Extraction

In [14], a method is used to extract the equivalent model of common mode response. The common mode equivalent lumped model of the proposed configuration is shown in Fig. 2. The common mode simulation results of each resonator can be matched to the one-pole Butterworth type low-pass response, which has 3-dB cutoff frequency in Fig. 3(a). C_p and L_p denote the gap capacitance between two sides of the slit and the equivalent inductance of the signal passing through the one DGS resonating unit. The extracted LC equivalent circuit can be found in [15] and are given bellow.

$$C_p = \frac{f_c}{4\pi Z_c}\left(\frac{1}{f_0^2 - f_c^2}\right) \tag{1}$$

$$L = \frac{1}{4\pi^2 f_0^2 C_p} \tag{2}$$

The mutual coupling is synchronous for two identical U-shaped or H-shaped resonators or identical dumb bell shaped resonator and is asynchronous between U- and H-shaped resonators or between unidentical dumb bell shaped resonators due to geometrical asymmetry. The magnetic coupling between any two resonators is dominant, f_{ei}

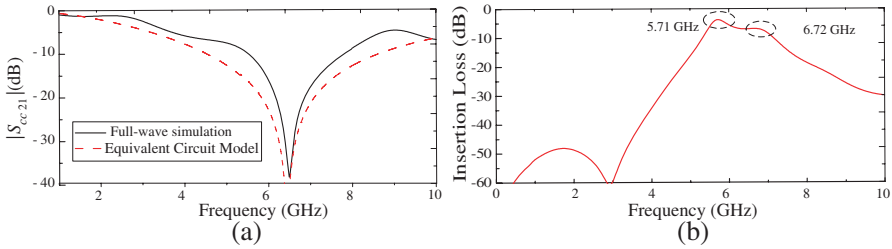

Figure 3. Common mode simulation to extract the equivalent lumped model (a) to extract the equivalent LC, (b) to extract the coupling coefficient k_m.

Table 1. Extracted parameters of equivalent lumped common mode model.

L_1	C_1	L_2	C_2	L_3	C_3	k_{m1}	k_{m2}
5.09 nH	0.06 pF	5.18 nH	0.08 pF	5.39 nH	0.146 pF	−0.057	−0.043
L_4	C_4	L_5	C_5	C_6	C_a	k_{m3}	k_{m4}
5.2 nH	0.116 pF	1.509 nH	0.658 pF	0.12 pF	4.7 nF	−0.135	−0.112

and f_{mi} denote two split resonant frequency due to the synchronous coupling, shown in Fig. 3(b); $f_{0(j+1)}$ and f_{0j} denote the self-resonant frequencies of each resonator without mutual coupling, where $f_{0(j+1)} > f_{0j}$, f_{j+1} and f_j denote two split resonant frequency due to the asynchronous coupling, where $f_{j+1} > f_j$. The magnetic coupling coefficient can be computed by the following formulas:

$$k_{mi} = \frac{L_{mi}}{l_i} = \frac{f_{ei}^2 - f_{mi}^2}{f_{ei}^2 + f_{mi}^2}, \quad i = 2, 4 \tag{3}$$

$$k_{mj} = \frac{L_{mj}}{L_j L_{j+1}} = \pm\frac{1}{2}\left(\frac{f_{0(j+1)}}{f_{0j}} + \frac{f_{0j}}{f_{0(j+1)}}\right) \times\sqrt{\left(\frac{f_{j+1}^2 - f_j^2}{f_{j+1}^2 + f_j^2}\right)^2 - \left(\frac{f_{0(j+1)}^2 - f_{0j}^2}{f_{0(j+1)}^2 + f_{0j}^2}\right)^2} \quad j = 1, 3 \tag{4}$$

The negative sign is chosen because the magnetic flux is mutually canceled for the same direction of the current flow on the defected ground plane.

Using this method, the equivalent model of Sections 2 and 3 in common mode can be extracted. The configuration of Section 1 is designed by a three-pole high-pass prototype according to the method [1]. So the equivalent model in common mode can be gained directly. The parameters of equivalent lumped common mode model are shown in Table 1.

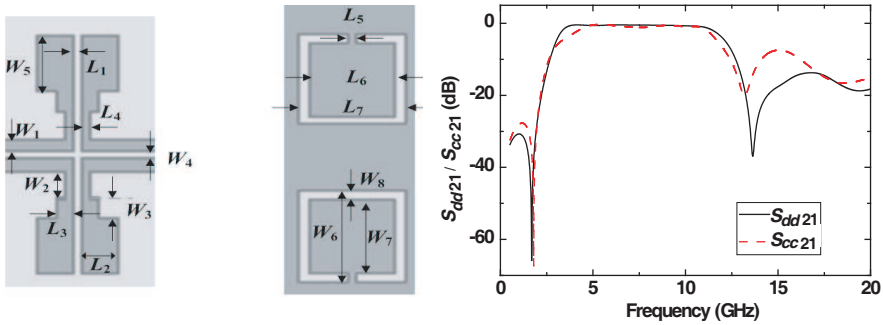

(a) (b) (c)

Figure 4. UWB filtering part of the balanced filter. (a) Its top view, (b) bottom view, and (c) the simulated S-parameters for differential and common modes. ($W_1 = 0.56\,\text{mm}$, $W_2 = 1.27\,\text{mm}$, $W_3 = 2.53\,\text{mm}$, $W_4 = 0.36\,\text{mm}$, $W_5 = 0.92\,\text{mm}$, $W_6 = 4.3\,\text{mm}$, $W_7 = 3.5\,\text{mm}$, $W_8 = 0.4\,\text{mm}$, $L_1 = 0.36\,\text{mm}$, $L_2 = 1.3\,\text{mm}$, $L_3 = 0.62\,\text{mm}$, $L_4 = 0.27\,\text{mm}$, $L_5 = 0.4\,\text{mm}$, $L_6 = 3.2\,\text{mm}$, and $L_7 = 4.0\,\text{mm}$.)

2.2. UWB Filtering Units for Differential Lines

As shown in Fig. 4, the UWB filtering part of our component contains two symmetrical units. Each unit is constructed by a pair of multimode resonators with a coplanar waveguide structure beneath them [15], which is utilized to provide a UWB bandpass characteristic for a single line of the differential pair. With this part, the UWB bandpass response with two transmission zeros is obtained for the differential mode. Obviously, the two UWB filtering units are independent with each other. Thus, the common-mode response is similar to the differential-mode one, as shown in Fig. 4(c). The relative permittivity of $\varepsilon_r = 4.3$, the loss tangent of $\tan\delta = 0.003$, and the thickness of $h = 0.41\,\text{mm}$. As shown in [14], the common-mode suppression level of UWB structure below 3 GHz is near 0 dB.

2.3. U- and H-Shaped DGSs for Lower Band Common-mode Suppression

In [14], U- and H-shaped DGSs are etched on the ground plane to suppress common-mode noise for GHz differential lines. Similar structures are utilized to improve the lower band common-mode rejection characteristic as the second part of the balanced filter, as shown in Fig. 5(a). This part consists of two U-shaped DGS resonators and an H-shaped one operating at lower band. The simulation of this part without capacitor loaded presents poor common mode suppression in lower passband as in [14]. Because ultra-wide stop-

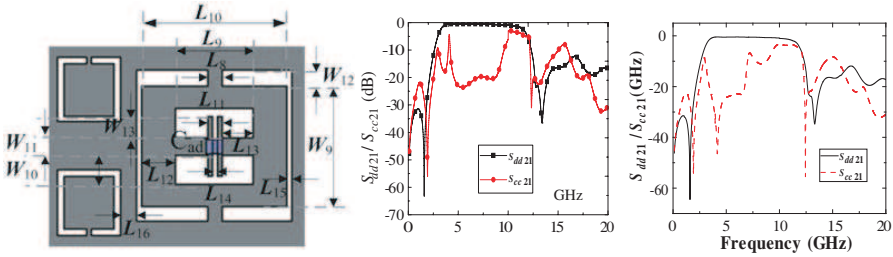

Figure 5. First and second parts of the balanced UWB BPF. (a) The configuration, and (b) the simulated results without capacitor. (c) The simulated results with capacitor. ($W_9 = 8.0\,\text{mm}$, $W_{10} = 1.9\,\text{mm}$, $W_{11} = 1.2\,\text{mm}$, $W_{12} = 1.0\,\text{mm}$, $W_{13} = 1.4\,\text{mm}$, $L_8 = 1.0\,\text{mm}$, $L_9 = 5.0\,\text{mm}$, $L_{10} = 9.4\,\text{mm}$, $L_{11} = 1.0\,\text{mm}$, $L_{12} = 2.2\,\text{mm}$, $L_{13} = 1.92\,\text{mm}$, $L_{14} = 0.36\,\text{mm}$, $L_{15} = 0.3\,\text{mm}$, and $L_{16} = 1.12\,\text{mm}$).

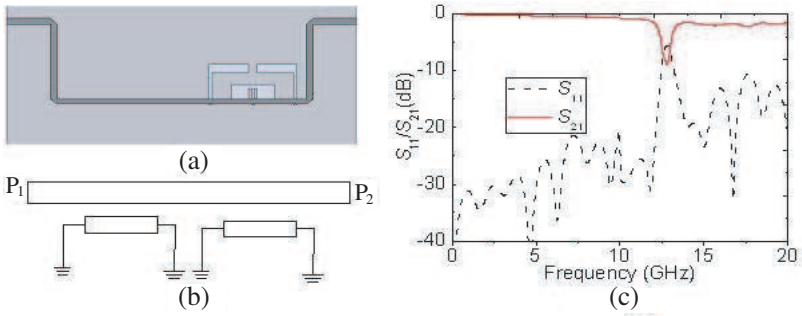

Figure 6. The differential response of DGS resonator in the Section 3. (a) The configuration, (b) the equivalent model, and (c) simulation.

band of common mode response is affected by resonation frequency of three LC resonator of UH-shaped DGS's equivalent circuit, and the resonation frequency of three LC resonator is affected by size of UH-shaped DGS. The wanted common mode rejection of lower-band of UWB needs lower resonation frequency of equivalent LC resonator, the lower resonation frequency of equivalent LC resonator needs larger size of DGS. To improve the common mode suppression in lower band and miniaturize the H-shaped DGS, a capacitor of 4.7 nF is loaded at its center. The simulated response of the first two parts is plotted in Fig. 5(c), with the optimized geometrical parameters also given.

The DGS resonators are seemed to be shorted to electric wall in differential mode response. The DGS resonators in Section 2 act mainly as two coupling bypass half-wavelength resonators shorted at two ends. The Section 2 with DGS resonators can be seemed

as two poles bandstop filter. The Fig. 6(c) presents the simulation results conforming to our analysis. The bandstop frequency is around 12.5 GHz.

2.4. Dumbbell-Shaped DGSs for Upper Band Common-mode Suppression

Patterned structure on top layer or ground is usually used to improve bandstop performance [16, 17]. In order to improve the performance of upper band common-mode suppression, a set of dumbbell-shaped DGS unit cells is designed as the third part of the proposed UWB balanced filter. As shown in Fig. 7(a), the dumbbell-shaped etched patterns [18] are located under both the two differential lines. The dominant mode of the DGS resonators is an even-mode, so they can provide a stopband at the dominant resonant frequency for the common mode. And their second resonant mode is an odd-mode, which will also produce a stopband at the second resonant frequency for the differential mode. Fig. 7(b) shows the optimized S-parameters of the cascading of the first and third parts of the proposed component. It is found that the common-mode suppression is achieved within not only the upper band of UWB but also the upper stopband, and the out-of-band rejection is also improved above 17 GHz for the differential mode filter.

The DGS resonators in Section 3 act mainly as four coupling bypass half-wavelength resonators shorted at two ends. The Section 3 with DGS resonators can be seemed as four poles bandstop filter (Figs. 8(a), (b)). The Fig. 8(c) presents the simulation results conforming to our analysis. The bandstop frequency is around 17 GHz.

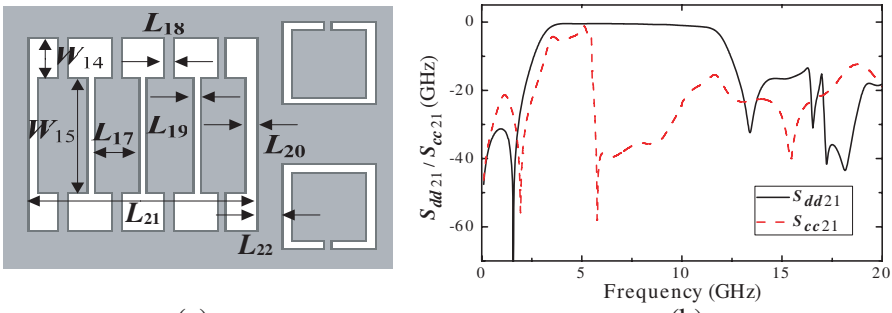

(a) (b)

Figure 7. First and third parts of the balanced UWB BPF. (a) The configuration, and (b) the simulated results. ($W_{14} = 2.0$ mm, $W_{15} = 3.0$ mm, $L_{17} = 2.0$ mm, $L_{18} = 0.4$ mm, $L_{19} = 0.3$ mm, $L_{20} = 0.4$ mm, $L_{21} = 10$ mm, $L_{22} = 0.88$ mm).

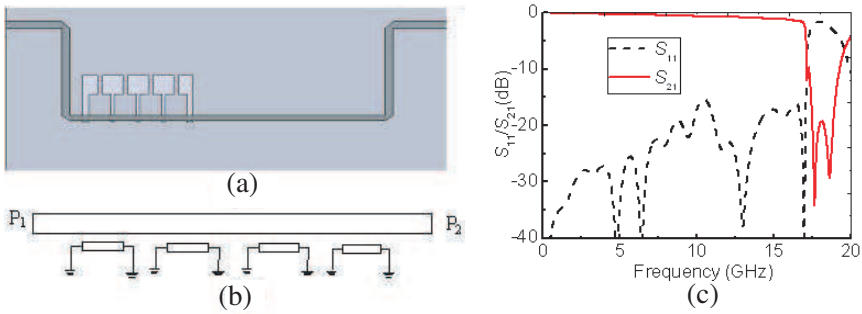

Figure 8. The differential response of DGS resonator in the Section 3. (a) The configuration, (b) the equivalent model, and (c) simulation.

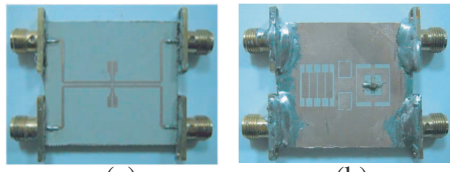

Figure 9. Photo of the fabricated filter prototype. (a) Its top view, and (b) bottom view.

The DGS resonators in Sections 2 and 3 provide two bandstop around 12.5 GHz and 17 GHz, which benefit the differential mode bandstop performance.

It is easy to understand that the common-mode suppression in the whole frequency range of interest can be implemented by using the U-/H-shaped DGSs and dumbbell-shaped ones together with the UWB filtering units, while the UWB bandpass characteristic of differential mode will not be degraded. So the proposed UWB balanced bandpass filter is a cascade of the three parts, as shown in Fig. 1.

3. RESULTS AND DISCUSSION

To validate our idea, a filter prototype is designed and fabricated on a Taconic TRF-43 substrate, with the relative permittivity of $\varepsilon_r = 4.3$, the loss tangent of $\tan\delta = 0.003$, and the thickness of $h = 0.41$ mm, as shown in Fig. 9. The overall size of the prototype is $26.2 \times 11.9\,\text{mm}^2$.

The balanced filter, as a four-port component, is measured by Agilent 8722ES vector network analyzer. Then, its S-parameters of differential and common modes are extracted by

$$S_{dd21} = S_{21} - S_{31} \tag{5}$$

$$S_{cc21} = S_{21} + S_{31} \tag{6}$$

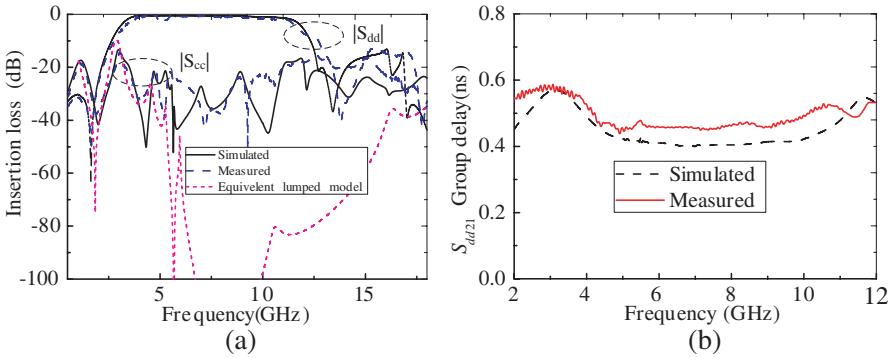

Figure 10. Insertion loss and group delay of the UWB balanced filter, (a) insertion loss, (b) group delay.

Table 2. Comparison to other published differential-mode ultrawide band filter.

Ref	[4]	[5]	[6]	[7]	this work
frequecy range in measurement	1-8 GHz	1-13 GHz	0-9 GHz	0-8 GHz	0-18 GHz
differential mode passband	2.7-5.3 GHz	2.9-10.7 GHz	2.8-5.3 GHz	1.6-4.37 GHz	3.54-10.6 GHz
differential mode passband insertion	0.5-2 dB	0.5-7dB	0.5-2.5 dB	1.19-2.05dB	0.11-2.50dB
common mode suppression level (passband)	>20 dB	>14 dB	>17 dB	>20 dB	>20 dB
common mode suppression level (lower stopband)	0-20 dB	0-20 dB	0-20 dB	>20 dB	>14.3 dB
common mode suppression level (upper stopband)	0-20 dB	0-20 dB	0-20 dB	>5 dB	>15.4 dB
compatible with microstrip	yes	yes	yes	No	yes

The extracted S-parameters of the prototype are plotted in Fig. 10(a), with its simulated results also provided for comparison. Good agreement is obtained between them. From 3.54 to 11.30 GHz, the insertion loss of differential mode is from 0.11 to 2.5 dB. The extracted 3-dB bandwidth of differential mode is from 3.52 to

11.40 GHz, slightly narrower than the simulated one from 3.24 to 11.67 GHz. The rejection level of common mode is better than 20 dB from 3.28 to 10.96 GHz in measurement, while the simulated 20-dB rejection band is from 3.51 to 10.98 GHz. The extracted common-mode suppressions in the lower and upper stopbands are better than 14.3 and 15.4 dB, respectively. As shown in Table 2, this work can not only directly connect to microstrip circuits but also suppress common mode noise to 14.3 dB both in lower and upper stopband. Fig. 10(b) shows the group delay of simulated and measured results. It is found the measured group delay is about 0.54 ns and the simulated group delay is about 0.46 ns at center frequency. The group delay is plain in pass band and almost not degraded within the passband.

4. CONCLUSION

In this work, a new UWB balanced BPF based on DGSs is designed. Since each differential line can act as the return path of current for the other one, the DGSs etched below the differential lines have little influence on the differential-mode response. The differential-mode and common-mode responses of the proposed component can be designed individually. The UWB bandpass characteristics for both modes are provided by a pair of multimode resonators on the top layer with two coplanar waveguides on bottom layer. The U-/H-shaped DGSs loaded with a capacitor and dumbbell-shaped ones suppress the common-mode noise within the whole frequency range of interest. The proposed UWB balanced BPF has a good performance of wideband common-mode suppression, which is demonstrated by the good agreement obtained between its measured and simulated S-parameters.

ACKNOWLEDGMENT

This work was supported by the National Basic Research Program of China under Grant of 2009CB320202, by the National Natural Science Foundation of China under Grant of 60821062, and by the National Natural Science Foundation of China under Grant of 61001014.

REFERENCES

1. Wu, C.-H., C.-H. Wang, and C. H. Chen, "Novel balanced coupled-line bandpass filters with common-mode noise suppression," *IEEE Trans. on Microw. Theory and Tech.*, Vol. 55, No. 2, 287–295, Feb. 2007.

2. Shi, J. and Q. Xue, "Novel balanced dual-band bandpass filter using coupled stepped-impedance resonators," *IEEE Microw. Wireless Compon. Lett.*, Vol. 20, No. 1, 19–21, Jan. 2010.
3. Shi, J. and Q. Xue, "Balanced bandpass filters using center-loaded half-wavelength resonators," *IEEE Trans. on Microw. Theory and Tech.*, Vol. 58, No. 4, 970–977, Apr. 2010.
4. Wu, S.-M., C.-T. Kuo, and C.-H. Chen, "Very compact full differential bandpass filter with transformer integrated using integrated passive device technology," *Progress In Electromagnetics Research*, Vol. 113, 251–267, 2011.
5. Wu, S.-M., C.-T. Kuo, P.-Y. Lyu, Y.-L. Shen, and C.-I. Chien, "Miniaturization design of full differential bandpass filter with coupled resonators using embedded passive device technology," *Progress In Electromagnetics Research*, Vol. 121, 365–379, 2011.
6. Wong, S.-K., F. Kung Wai Lee, S. Maisurah, M. N. B. Osman, and S.-J. Hui, "Design of 3 to 5 GHz cmos low noise amplifier for ultra-wideband (UWB) system," *Progress In Electromagnetics Research C*, Vol. 9, 25–34, 2009.
7. Sayidmarie, K. H. and Y. A. Fadhel, "Self-complementary circular disk antenna for UWB applications," *Progress In Electromagnetics Research C*, Vol. 24, 111–122, 2011.
8. Diet, A. and N. Ribiere-Tharaud, "An "F-gain" antenna for UWB-RFID," *Progress In Electromagnetics Research C*, Vol. 20, 111–123, 2011.
9. Najam, A. I., Y. Duroc, and S. Tedjni, "UWB-MIMO antenna with novel stub structure," *Progress In Electromagnetics Research C*, Vol. 19, 245–257, 2011.
10. Lim, T.-B. and L. Zhu, "A differential-mode wideband bandpass filter on microstrip line for UWB application," *IEEE Microw. Wireless Compon. Lett.*, Vol. 19, No. 10, 632–634, Oct. 2009.
11. Lim, T.-B. and L. Zhu, "Differential-mode ultra-wideband bandpass filter on microstrip line," *Electron. Lett.*, Vol. 45, No. 22, 1124–1125, Oct. 2009.
12. Lim, T.-B and L. Zhu, "Highly selective differential-mode wideband bandpass filter for UWB application," *IEEE Microw. Wireless Compon. Lett.*, Vol. 21, No. 3, 133–135, Mar. 2011.
13. Chen, J.-X. and Q. Xue, "A novel differential bandpass filter based on double-sided parallel-strip line dual-mode resonator," *Microw. Opt. Tech. Lett.*, Vol. 50, No. 7, 1733–1735, Jul. 2008.
14. Wu, S.-J., C.-H. Tsai, and T.-L. Wu, "A novel wideband common-mode suppression filter for GHz differential signals using coupled

patterned ground structure," *IEEE Trans. on Microw. Theory and Tech.*, Vol. 57, No. 4, 848–855, Apr. 2009.

15. Ahn, D., J. S. Park, C. S. Kim, J. Kim, Y. Qian, and T. Itoh, "A design of the low-pass filter using the novel microstrip defected ground structure," *IEEE Trans. on Microw. Theory and Tech.*, Vol. 49, No. 1, 86–93, Jan. 2001.
16. Lee, J.-K. and Y.-S. Kim, "Ultra-wideband bandpass filter with improved upper stopband performance using defected ground structure," *IEEE Microw. Wireless Compon. Lett.*, Vol. 20, No. 6, 316–318, Jun. 2010.
17. Tang, I.-T., D.-B. Lin, C.-M. Li, and M.-Y. Chiu, "Compact pentagon ultra-wide band-pass filter with good out-of-band performance," *Journal of Electromagnetic Waves and Applications*, Vol. 23, No. 13, 1695–1706, 2009.
18. Liu, W. T., C. H. Tsai, T. W. Han, and T. L. Wu, "An embedded common-mode suppression filter for GHz differential signals using periodic defected ground plane," *IEEE Microw. Wireless Compon. Lett.*, Vol. 18, No. 4, 248–250, Apr. 2008.